

Size effects and strain state of $\text{Ga}_{1-x}\text{In}_x\text{As}/\text{GaAs}$ multiple quantum wells: Monte Carlo study

J. T. Titantah,¹ D. Lamoen,¹ M. Schowalter,² and A. Rosenauer²

¹*EMAT, Universiteit Antwerpen, Groenenborgerlaan 171, 2020 Antwerpen, Belgium*

²*Institut für Festkörperphysik, Universität Bremen, D 28359 Bremen, Germany*

(Received 22 July 2008; revised manuscript received 22 September 2008; published 28 October 2008)

The effect of the size of the GaAs barrier and the $\text{Ga}_{1-x}\text{In}_x\text{As}$ well on the structural properties of a $\text{Ga}_{1-x}\text{In}_x\text{As}/\text{GaAs}$ multiple quantum well structure is investigated using the Metropolis Monte Carlo approach based on a well-parametrized Tersoff potential. It is found that within the well the Ga-As and In-As bond lengths undergo contractions whose magnitude increases with increasing In content in sharp contrast with bond-length variations in the bulk $\text{Ga}_{1-x}\text{In}_x\text{As}$ systems. For fixed barrier size and In content, the contraction of the bonds is also found to increase with increasing size of the well. Using the local atomic structure of the heterostructures, a more local analysis of the strain state of the systems is given and comparison with the prediction of macroscopic continuum elasticity theory shows deviations from the latter.

DOI: [10.1103/PhysRevB.78.165326](https://doi.org/10.1103/PhysRevB.78.165326)

PACS number(s): 68.65.Fg, 81.07.Bc, 68.37.Lp, 61.46.-w

I. INTRODUCTION

$\text{Ga}_{1-x}\text{In}_x\text{As}$ is currently being used as the active region of quantum wells (QW) for lasers operating at wavelengths ranging from 1.6 to 2.1 μm .¹ Such lasers are mostly useful as infrared lasers in spectroscopy and medicine. Nitrogen containing $\text{Ga}_{1-x}\text{In}_x\text{As}$ can be tailored to operate at wavelengths of 1.3–1.55 μm which are most appropriate in optical fiber applications² for telecommunication.³ High performance single QW (SQW) operating at 1.24 μm have been realized but multiple QWs (MQWs) are more desirable because of their high thermal stability and longer wavelength.¹

In order to achieve wavelengths of up to 1.2 μm , high indium content $\text{Ga}_{1-x}\text{In}_x\text{As}$ MQW are used. Such systems are characterized by high strain levels.⁴ The sizes of the barrier (in most cases GaAs or InP) and the well in the multistack become important factors that should be carefully chosen in order to optimize the optical quality of the device. Most of the studies that have been carried out hardly investigate the effect of the barrier size on the properties of the device; they often emphasize the effect of the well size² although it has been suggested that strain balancing using tensile strained barriers could be of help in improving the quality of MQWs (see Ref. 5 and references therein). The amount of strain in both the barrier and the well depends on the barrier and/or well size.⁶ Amiotti *et al.*⁵ demonstrated how the quality of MQWs of $\text{Ga}_{1-x}\text{In}_x\text{As}$ on InP barrier is affected by the size of the InP layer. Mitsuhashi *et al.*⁷ showed how the photoluminescence intensity of a 1.65% strained InGaAs MQW changes as the strain within the barrier is changed. A complete understanding of the local atomic structure (e.g., bond lengths) across these heterostructures is still lacking.

In this work we perform a thorough theoretical investigation of the effect of the size of both the barrier and the well on the structural properties of MQWs of $\text{Ga}_{1-x}\text{In}_x\text{As}$ on GaAs barriers. In particular, we focus on the effect on bond lengths and the strain within the MQW.

II. THEORETICAL METHOD

Computer models of MQWs constituting $\text{Ga}_{1-x}\text{In}_x\text{As}$ layers of various thicknesses on GaAs(001) barriers were con-

structed and the resulting structures were relaxed using the zero pressure Metropolis Monte Carlo (MC) procedure in periodic boundary conditions (PBC). The in-plane (the xy plane) supercell lattice parameter was fixed at 28.3 Å. The use of three-dimensional periodic boundary conditions implies that the systems considered here are infinite stacks of multiple quantum wells. During the MC relaxation the perpendicular (with respect to the interface) box size was allowed to fluctuate but the in-plane box size was fixed to that of the GaAs barrier. Indium concentrations varying from 20% to 80% were considered and for each In content a random distribution of In atoms was assumed. The MC procedure used here is described as follows: each atom is given a random displacement and the total-energy change in the system ΔE is evaluated. This position is accepted or rejected according to the probability $P = \min[1, \exp(-\Delta E/k_B T)]$, where k_B is Boltzmann's constant and T is the temperature in kelvin. After all atoms have moved, the volume of the system is changed by randomly changing the perpendicular box length, then ΔE and the ratio of the new and old box sizes R is obtained. The box size is accepted or rejected with the probability $W = \min\{1, \exp[-\Delta E/k_B T + (N-2)\log R]\}$, where N is the number of particles in the system. We use the Tersoff empirical potential⁸ that was recently parametrized by us⁹ using accurate *ab initio* energies and the elastic constants of the corresponding binary crystals.

III. RESULTS

The results obtained in this work have been checked for any influence of the periodic boundary conditions used in the simulation of the nanostructured systems. In Fig. 1 the distributions of the Ga-As bond length and the lattice parameter perpendicular to the GaInAs/GaAs interface are shown for 40% and 80% In containing GaInAs quantum wells. For each case, periodic boundary conditions were implemented in two ways: (1) a supercell with only a single QW and (2) a supercell with two QWs with the same indium spatial distribution were considered. Within the error bars, which are obtained by analyzing the data of the entire MC relaxation run in terms of five blocks of independent data, it can be seen

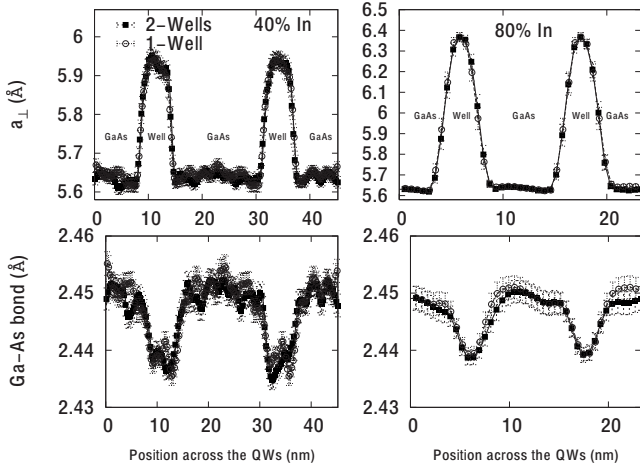


FIG. 1. Effect of periodic boundary conditions on the structural properties: the perpendicular lattice parameter (upper panels) and Ga-As bond-length (lower panels) distribution across the quantum wells for (left) 20 MLs of 40% In containing QW on 60 MLs of GaAs and (right) 12 MLs of 80% In containing QW on 28 MLs of GaAs. Two types of supercells are considered: one containing only one QW and the other with two QWs. Error bars are obtained from five-block data analysis of the entire MC moves. Within every layer each atom is considered and the average radius (averaged over four distances for in-plane lattice parameter and two distances for out-of-plane lattice parameter) of the fourth atomic coordination shell around this atom is retained as the local lattice parameter.

that both properties do not depend on the number of the QWs in the supercell. We also checked the effect of the PBC as applied to the lateral dimensions of the simulation cell and found little or no effect on the properties.

A. Variation in the Ga-As and In-As bond lengths with well size

A typical Ga-As bond-length profile, nearest-neighbor correlation function, and In fraction changes across the well are shown in Fig. 2 for a 40% In, 11.4 nm well on 23 nm barrier where it is seen that the bond length shrinks within the well. The effect of well size on the average Ga-As bond length is investigated and the results in Figs. 3–6 show monolayer (ML) by monolayer dependence of the average Ga-As bond length. The shrinking of the Ga-As bonds within the wells is in very good agreement with measurements.^{10–12} In particular, the values of 2.442 Å for the 2.3 nm well (8 MLs on 31.7 nm barrier) and 2.441 Å for the 3.4 nm well (12 MLs on 30 nm barrier) both with 20% In fraction are in excellent agreement with the value of 2.442 Å as obtained in Ref. 13 for a $\text{Ga}_{0.78}\text{In}_{0.22}\text{As}$ layer buried in GaAs. The bond lengths in the barrier also depend on the sizes of the well and the barrier.

The plot of the Ga-As and In-As bond lengths as a function of In fraction and for various well sizes is shown in Fig. 7. The total size of the well and the barrier was fixed at 120 MLs. The well sizes were 8, 12, 20, 32, and 40 MLs, respectively. The dependence of both Ga-As and In-As bond lengths on In content is nonlinear, showing negative bowing especially for large wells. They both have the form $r_\alpha(x, L)$

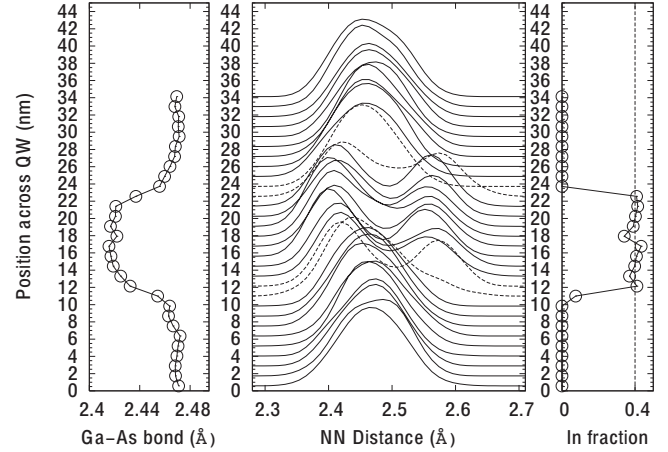


FIG. 2. Left: Variation in the Ga-As bond length (in angstrom) across the well of a multiwell $\text{Ga}_{1-x}\text{In}_x\text{As}$ system from the GaAs region through the $\text{Ga}_{1-x}\text{In}_x\text{As}$ layer and back to the GaAs region. Middle: Nearest-neighbor pair-correlation function as a function of bond length (in angstrom) showing the bimodal bond-length distribution within the well. Ga-As bond length shows up at ~ 2.4 Å and that of In-As at ~ 2.6 Å. Right: Variation in In content for the nominal 40% In containing $\text{Ga}_{1-x}\text{In}_x\text{As}$ quantum well. Well width is ~ 11.4 nm and the GaAs barrier is ~ 23 nm thick.

$= (1-x)r_\alpha^0 + xr_\alpha^1(L) + x(1-x)\delta_\alpha(L)$, where α is GaAs (InAs) and r_α^0 (r_α^1) is the α -type bond length in dilute In (Ga) well, respectively. While r_α^0 is independent of well size, r_α^1 decreases with increasing well size. The bowing parameter $\delta_\alpha(L)$ decreases with increasing well size, being positive for thin wells and negative for large wells. For very thin wells both Ga-As and In-As bond lengths are almost constant. The almost constant bond lengths in thin wells are in good agree-

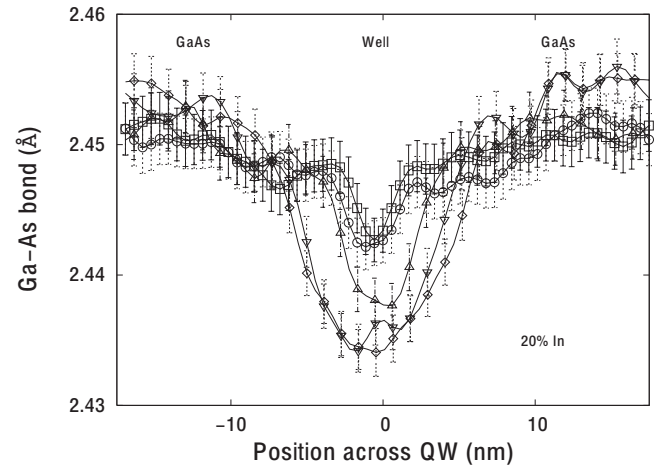


FIG. 3. Ga-As bond-length distribution across the well for 20% In content and various well thicknesses (bond lengths are averaged over all the atoms within slices of thickness ~ 2.9 Å). The total size of the well and barrier is fixed at 120 MLs while the well sizes are set to 8 (rectangles), 12 (circles), 20 (triangles), 32 (inverted triangles), and 40 (diamonds) MLs. Within the well and for each In content, the Ga-As bond length decreases as the well size increases from 8 MLs through 12, 20, 32, and 40 MLs. Error bars are obtained from five-block data analysis of the entire MC moves.

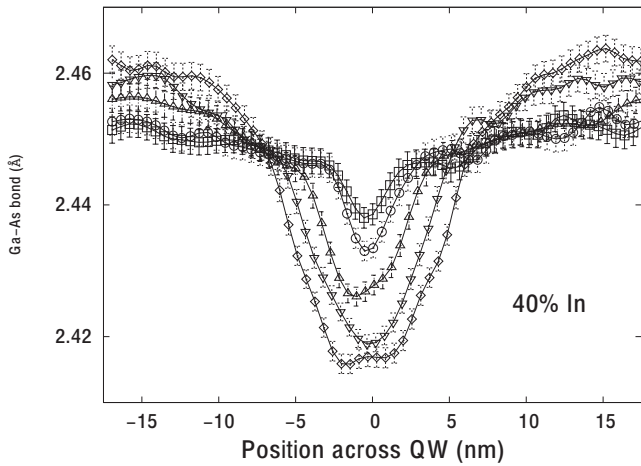


FIG. 4. Ga-As bond-length distribution across the well for 40% In content and various well thicknesses (bond lengths are averaged over all the atoms within slices of thickness ~ 0.29 nm). The total size of well and barrier is fixed at 120 MLs while the well sizes are set to 8 (rectangles), 12 (circles), 20 (triangles), 32 (inverted triangles), and 40 (diamonds) MLs. Within the well and for each In content, the Ga-As bond length decreases as the well size increases from 8 MLs through 12, 20, 32, and 40 MLs. Error bars are obtained from five-block data analysis of the entire MC moves.

ment with other findings.^{10,12} As expected, the value of the Ga-As bond length for dilute In limit, r_{GaAs}^0 , is exactly equal to that of the bulk GaAs bond length for all well sizes [$r_{\text{GaAs}}^0 = (2.448 \pm 0.002)$ Å]. In this limit that of In-As [$r_{\text{InAs}}^0 = (2.583 \pm 0.004)$ Å] is in excellent agreement with the reported value of (2.581 ± 0.004) Å obtained for strained 21.5% In content InGaAs layers.¹¹ The present work also compares well with the random-cluster calculations of bond

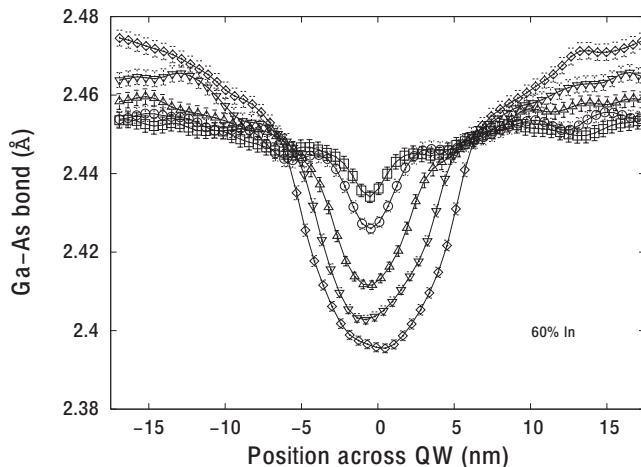


FIG. 5. Ga-As bond-length distribution across the well for 60% In content and various well thicknesses (bond lengths are averaged over all the atoms within slices of thickness ~ 0.29 nm). The total size of well and barrier is fixed at 120 MLs while the well sizes are set to 8 (rectangles), 12 (circles), 20 (triangles), 32 (inverted triangles), and 40 (diamonds) MLs. Within the well and for each In content, the Ga-As bond length decreases as the well size increases from 8 MLs through 12, 20, 32, and 40 MLs. Error bars are obtained from five-block data analysis of the entire MC moves.

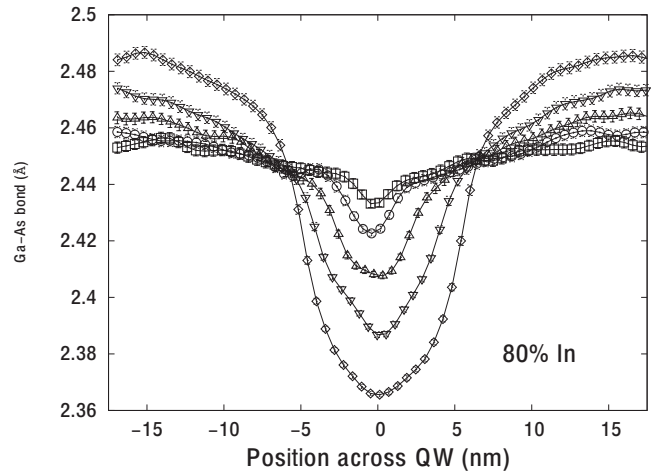


FIG. 6. Ga-As bond-length distribution across the well for 80% In content and various well thicknesses (bond lengths are averaged over all the atoms within slices of thickness ~ 0.29 nm). The total size of well and barrier is fixed at 120 MLs while the well sizes are set to 8 (rectangles), 12 (circles), 20 (triangles), 32 (inverted triangles), and 40 (diamonds) MLs. Within the well and for each In content, the Ga-As bond length decreases as the well size increases from 8 MLs through 12, 20, 32, and 40 MLs. Error bars are obtained from five-block data analysis of the entire MC moves.

lengths in strained Ga_{1-x}In_xAs alloys on GaAs using the Keating valence-force field.¹⁰ However, the effect of well size was not addressed in that work. Hellmann-Feynman force calculations have been used to study the effects of external strain on a Ga_{1-x}In_xAs epilayer in a Ga_{1-x}In_xAs/GaAs heterostructure.¹⁴ While the Ga-As bond lengths obtained in that work showed similar behavior with the one presented in this work, the In-As bond lengths were underestimated to be 2.54 Å for a 25% In system.

B. Effect on strain

The strains within the systems have been evaluated from the local lattice parameters. As was pointed out by Massies and Grandjean¹⁵ for a better understanding of the strained

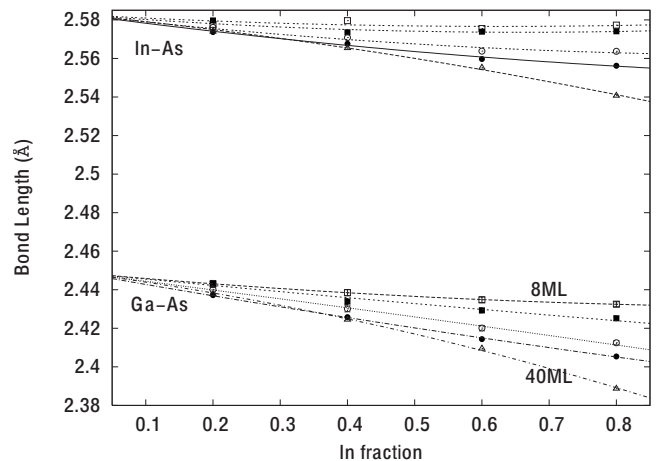


FIG. 7. Ga-As and In-As bond lengths in the well for various well sizes. Note the almost constant bond lengths for thin wells.

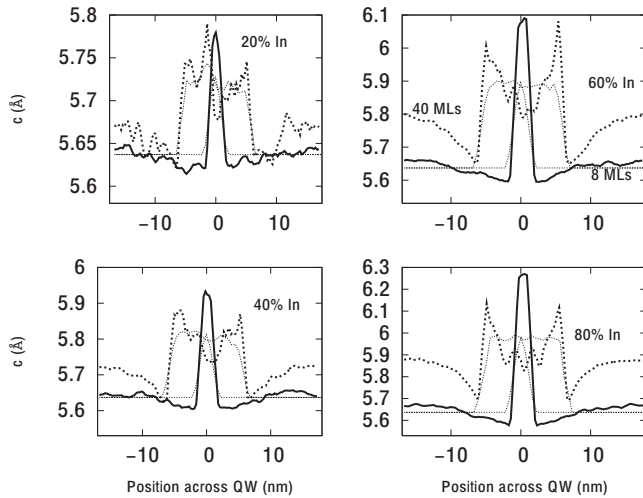


FIG. 8. Variation in the perpendicular lattice parameter across the well of a multiwell $\text{Ga}_{1-x}\text{In}_x\text{As}$ system from the GaAs region through the $\text{Ga}_{1-x}\text{In}_x\text{As}$ layer and back to the GaAs region. The full lines correspond to 8 ML wells, the dotted lines are for 40 ML wells, and the thin dotted lines are deduced from the Vegard's law $a_f = (1-x)a_{\text{GaAs}} + xa_{\text{InAs}}$. Numerical errors range from 0.005 to 0.01 Å. The total size of the well and the barrier is fixed at 120 MLs. Within every layer each atom is considered and the average radius (averaged over four distances for in-plane lattice parameter and two distances for out-of-plane lattice parameter) of the fourth atomic coordination shell around this atom is retained as the local lattice parameter.

state of the epilayers, it is important to consider the local lattice parameter rather than the macroscopic crystal lattice parameter. Atomistic calculations are, therefore, most appropriate to adequately study the strain profile in InGaAs/GaAs heterostructures.^{16–18} In this work, the local lattice parameter was determined by exploiting the fact that the radius of the fourth coordination shell of atoms in the zinc-blende structure is equal to the lattice parameter. Within every layer each atom is considered and the average radius (averaged over four distances for in-plane lattice parameter and two distances for out-of-plane lattice parameter) of the fourth atomic coordination shell around this atom is thus retained as the local lattice parameter accommodating the atom. In Fig. 8 the variation in the lattice parameter perpendicular to the interface is presented and this parameter within the barrier and the well depends on the thicknesses of the well and/or the barrier. At the GaInAs/GaAs interface on the GaAs side it decreases to lower values within 2–4 monolayers while on the InGaAs side there is a tetragonal distortion within 2–4 MLs. In the middle of the well, the perpendicular lattice parameter increases with increasing In content but remains smaller than the values at the edges of the well. These results are in agreement with other calculations.^{17–20} It is important to note here that within the barrier the perpendicular lattice parameter depends on both the In content and the well and barrier sizes. Thus it is not only the active layer that is strained but also the barrier layer. This is consistent with the findings of a calculation using the anharmonic Keating valence-force field¹⁷ on MQWs in which it was found that the presence of a GaInAs layer inside a GaAs matrix can

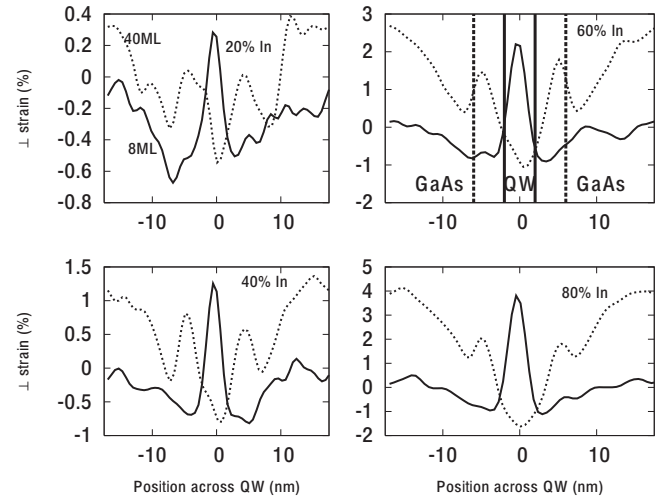


FIG. 9. Perpendicular strain variation across the well of a multiwell $\text{Ga}_{1-x}\text{In}_x\text{As}$ system. The dotted lines correspond to 40 ML wells on 80 ML GaAs while the full lines are for 8 ML well on 112 ML GaAs. The vertical lines in the upper right panel show the extent of the quantum well: dashed lines for the 40 ML well and full lines for the 8 ML well. The perpendicular strain is defined as $\epsilon_{\perp} = (a_{\perp} - a_f) / a_f$, where a_f is the lattice parameter of the bulk material with similar composition and a_{\perp} is the local lattice parameter perpendicular to the interface. The error bars on the strains range from 0.1% to 0.15%. This means that the fluctuation at about 10 nm for the 20% In containing large well is a numerical noise.

introduce strain as deep as 15 nm into the GaAs buffer. It is also consistent with a barrier and well thicknesses related relaxation mechanism within the active layer.⁶

The uniaxial strain components of the layer relative to the bulk materials are: $\epsilon_{\perp} = (a_{\perp} - a_f) / a_f$ and $\epsilon_{\parallel} = (a_{\parallel} - a_f) / a_f$, where a_f is the lattice parameter of the bulk material with similar composition, and a_{\perp} and a_{\parallel} are the local lattice parameters perpendicular and parallel to the interface, respectively. To a good level of accuracy, and as was recently demonstrated by us,⁹ a_f is determined by Vegard's law $a_f = (1-x)a_{\text{GaAs}} + xa_{\text{InAs}}$. Using the lattice parameters determined above and the values of a_f as dictated by the In fraction at each layer, the fractional perpendicular strain is calculated and displayed in Fig. 9 for two well sizes of 8 and 40 MLs on 112 and 80 MLs of GaAs barriers, respectively. We have found that wells larger than 5 nm are compressively strained while smaller wells are tensile strained.

It is important to point out the size dependence of the perpendicular strain as this is of relevance in interpreting the observed optical changes in MQWs subject to various physical and/or chemical conditions such as thermal treatment and/or chemical composition alterations (e.g., nitrogen insertion). For the smaller well size of 8 MLs, the well is under a tensile strain while the interface on the GaAs side is compressively strained. The larger well of 40 MLs shows quite a different scenario; an interface region of about 2–4 MLs where strong variation in the strain is recorded and the center of the well is under compressive strain with respect to the bulk material.

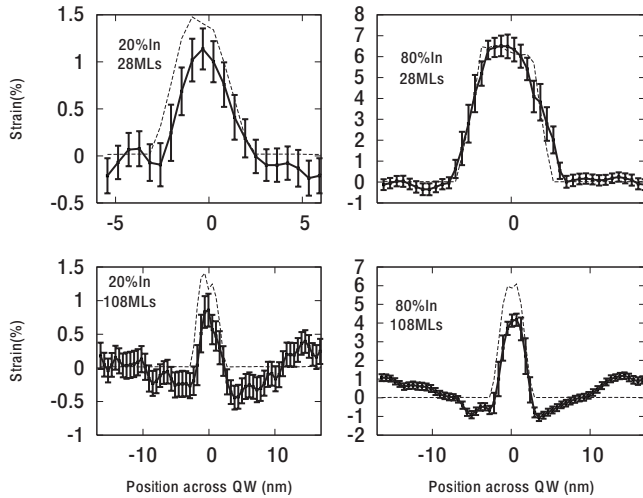


FIG. 10. Perpendicular strain variation across the well of a multiwell $\text{Ga}_{1-x}\text{In}_x\text{As}$ system from the GaAs region through the $\text{Ga}_{1-x}\text{In}_x\text{As}$ layer and back to the GaAs region: comparison between calculations (full lines) and the prediction of the continuum elasticity theory (thin dashed lines). Error bars are obtained from five-block data analysis of the entire MC moves.

C. Comparison with the prediction of the continuum elasticity theory

Since the lattice parameter of bulk $\text{Ga}_{1-x}\text{In}_x\text{As}$ is always larger than that of GaAs, elasticity theory will always predict a tetragonal extension (in the growth direction) of $\text{Ga}_{1-x}\text{In}_x\text{As}$ films grown on GaAs substrate because of the in-plane compressive strain. However, our atomistic model shows that this is only true for thin QWs (≤ 5 nm). Thicker QWs show a clear deviation from the elasticity theory as shown in Fig. 9. This deviation is due to local relaxation of the GaInAs lattice.

In order to compare these strains with the prediction of continuum elasticity (CE) theory, we have performed calculations on 3.4 nm (12 MLs) wells on GaAs barriers of two different sizes [28 MLs (~ 7.9 nm) and 108 MLs (~ 30.5 nm), respectively]. As was shown earlier, this well size is smaller than the critical thickness above which strain relaxation is found to occur. Two In fractions are considered: $x=0.20$ and $x=0.80$. The CE theory predicts that $\epsilon_{\perp}(x) = -[2c_{12}(x)/c_{11}(x)]\epsilon_{\parallel}$, where c_{11} and c_{12} are the elastic constants of the bulk material of similar In content. For GaAs we used $c_{11}=118$ GPa and $c_{12}=52$ GPa, and for InAs values of 83 and 48 GPa are used, respectively.⁹ Figure 10 compares the perpendicular strain as obtained from the local lattice parameters and the strain deduced from the CE theory. For the elastic constants we use the values $c(x)=(1-x)c_{\text{GaAs}}+xc_{\text{InAs}}$. As can be seen in Fig. 10, the finite size of the GaAs barrier causes a strain of the GaAs layer. For the high In content, the middle of the larger barrier is tensile strained while toward the edge of the well it is compressively strained. Apart from the case of thin wells on GaAs barriers where the prediction of the CE theory is recovered, deviations from the prediction of the CE theory are found for all the other systems, in accordance with other atomistic calculations on InAs/GaAs (Ref. 21) and CdSe/ZnSe (Ref. 22)

quantum dots, and analytical transmission electron microscopy (TEM) measurements on GaInAs islands.²³ The uniaxial strain value of 6.3% in the 80% In MQW on 28 ML GaAs is comparable with the value of 6.5% obtained for thin InAs islands on GaAs (Ref. 15) and is consistent with a biaxial strain value of 12.6% of a ML of InAs sandwiched in GaAs as measured by TEM.²⁴

The size dependent bond length and strain (in the well and the barrier) elaborated upon in this work may offer additional explanation to the changes in the optoelectronic properties of MQW; in particular the shift in photoluminescence energies on thermal annealing and/or the insertion of nitrogen. The need for an alternative explanation is supported by some experimental and theoretical findings. For example, Mitsu-hara and co-workers¹⁷ showed that the photoluminescence intensity of MQW is strongly affected by the strain level of the well and, using TEM measurements, they also found that the structural properties of MQW are sensitive to the barrier strain.¹ Recently, Ishikawa *et al.*²⁵ showed that the cathodoluminescence intensity and peak energy of $\text{Ga}_{0.64}\text{In}_{0.36}\text{As}_{0.955}\text{N}_{0.045}$ depend on the size of the QW. The enhanced intensity of the larger well was attributed to possible enhancement of electron and hole captures in the well. Ni *et al.*² also attributed the temperature-dependent photoluminescence peak energies and intensities to lattice dilation and electron-lattice interaction. Also a huge part of the bowing of band gaps in $\text{GaAs}_{1-x}\text{N}_x$ systems (giant reduction in band gap) has been shown²⁶ to result from the static atomic displacements around N, suggesting that bond-length changes in such systems could cause major changes in their optical properties, as was reported in Ref. 15, and also pointed out by Boscherini *et al.*²⁷

It is worth noting here that we expect that, for large enough barriers, there should exist a well size beyond which the properties of the well tend to those of the bulk material of similar In content. We considered 40% In containing $\text{Ga}_{1-x}\text{In}_x\text{As}$ wells of various thicknesses on 160 MLs (~ 46 nm) of GaAs. In Fig. 11 we show (a) the Ga-As and (b) In-As bond lengths, (c) the difference between the energy per atom of the well and that of the bulk sample with similar In content ($\Delta\text{Energy}=E_{\text{well}}-E_{\text{bulk}}$), and (d) the perpendicular strain within the well and the barrier. Even for wells as large as 60 MLs, the properties still deviate drastically from the bulk values. Wells larger than 10 MLs (~ 3 nm) are under compressive strain and are energetically less favorable than the bulk material while the barrier is under tensile strain.

D. Choice of the parameters of the potential

Recently a different set of parameters of the Tersoff potential was obtained after extensive fits of the properties of the various phases of In, Ga, GaAs, and InAs.²⁸ This set of parameters was shown to accurately reproduce the elastic properties of the zinc-blende binary GaAs and InAs crystals. It has not yet been used to simulate strained systems such as QWs. We have used these parameters to simulate structural changes in both bulk and strained GaInAs systems. We have found that for bulk GaInAs systems the average bond length, the Ga-As and In-As bond lengths, reproduce the z shape^{9,13}

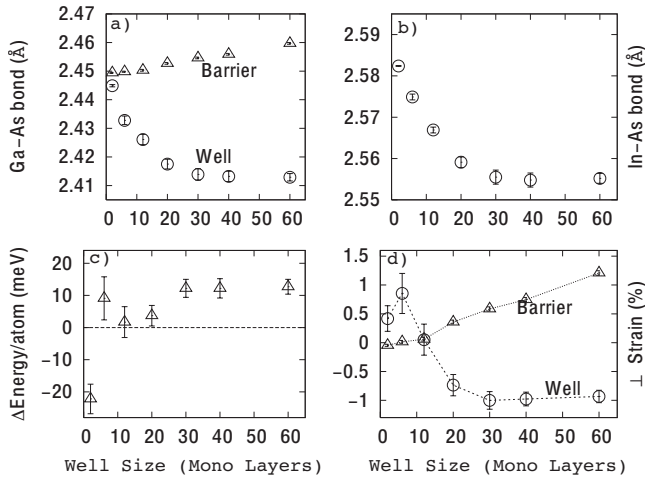


FIG. 11. Effect of well size on the properties of a 40% $\text{Ga}_{1-x}\text{In}_x\text{As}$ MQW on 160 ML GaAs barrier: (a) Ga-As bond length in the barrier and the well, (b) In-As bond length, (c) difference between the energy per atom of the well and that of the bulk material of similar In content, and (d) the perpendicular strain within the well and the barrier.

that is characteristic of the dependence of bond lengths on In content for bulk GaInAs systems. However, we see that the Ga-As bond length in the dilute Ga limit is overestimated to 2.54 Å while the In-As bond in the dilute In limit is underestimated to 2.54 Å (see Fig. 12) which are in contrast with the results of Titantah *et al.*⁹ and the measurements of Ref. 29. When we use this set of parameters²⁸ to simulate the structural properties of strained 40% In content GaInAs QW, the results in Fig. 13 are obtained. As can be seen, the Ga-As bond length and the perpendicular lattice parameters are consistently larger than the ones obtained using the parameters of Titantah *et al.*⁹ From Fig. 13 we also notice that the pa-

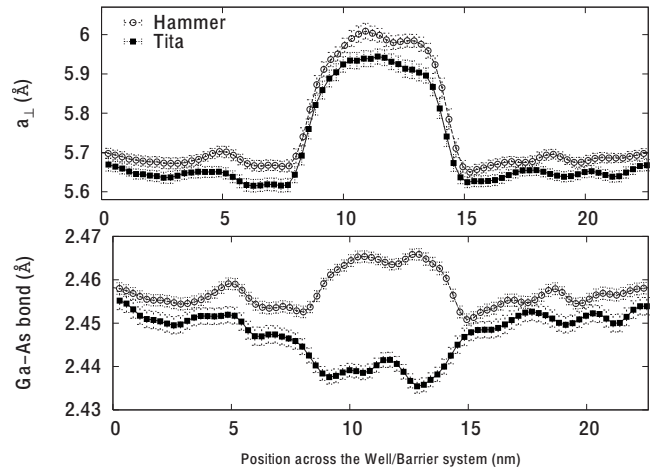


FIG. 13. The lattice parameter and bond-length distributions for two parametrizations of the Tersoff potential: (a) the parametrization of Hammerschmidt *et al.* (Hammer) (Ref. 28) and (b) that of Titantah *et al.* (Tita).⁹

rametrization of Hammerschmidt *et al.*²⁸ does not show the experimentally observed bond-length contraction.²⁹

IV. SUMMARY

We have demonstrated that the structural properties of MQWs depend on the size of both the barrier and the well and, in particular, that the Ga-As and In-As bond lengths depend strongly on the well and barrier sizes. The strain state, which is known to affect the optoelectronic properties of III-V MQWs, is also found to depend on both well and barrier sizes, and we have demonstrated the limitations of the continuum elasticity theory in explaining the strain state of the InGaAs/GaAs quantum wells. This study suggests the

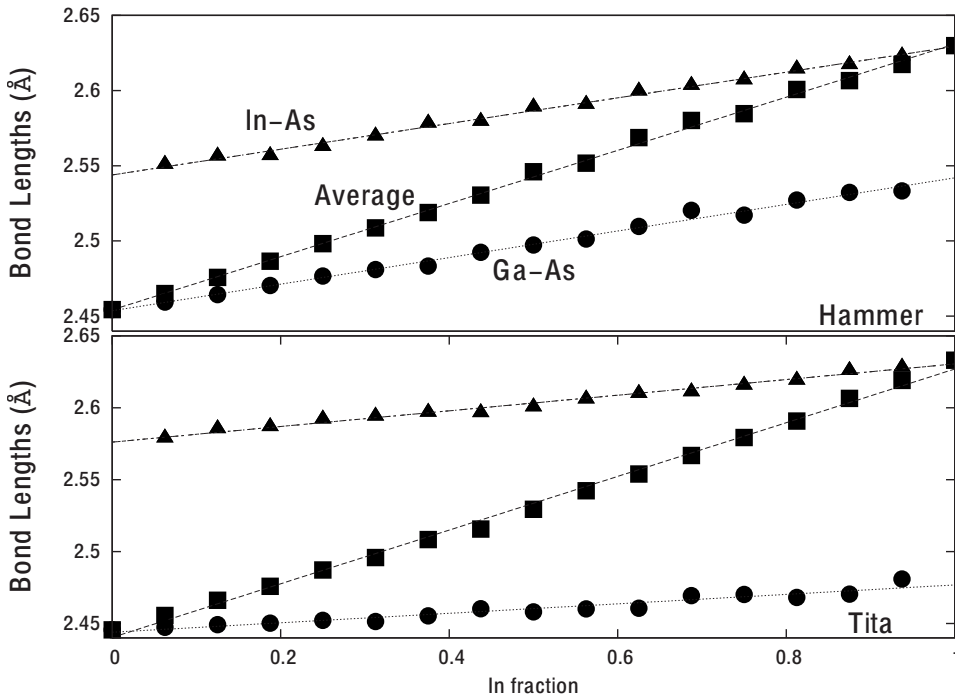


FIG. 12. The average bond length, and In-As and Ga-As bond-length variation with In content for two sets of the parameters of the Tersoff potential: that of Hammerschmidt *et al.* (Hammer) (Ref. 28) and that of Titantah *et al.* (Tita).⁹ Calculations were done on 512 atoms bulk GaInAs systems.

necessity of careful choice of both well and barrier sizes for optimal device quality.

ACKNOWLEDGMENTS

We acknowledge financial support from the FWO-Vlaanderen under Contract No. G.0425.05 and the Deutsche

Forschungsgemeinschaft under Contract No. RO2057/4-1. The authors also acknowledge financial support from the European Union under the Framework 6 program under a contract for an Integrated Infrastructure Initiative, Reference 026019 ESTEEM. Calculations have been performed on the CalcUA supercomputer of the University of Antwerp.

-
- ¹M. Mitsuhashi, M. Ogasawara, M. Oishi, and H. Sugiura, *Appl. Phys. Lett.* **72**, 3106 (1998).
- ²H. Q. Ni, Z. C. Niu, X. H. Xu, Y. Q. Xu, W. Zhang, X. Wei, L. F. Bian, Z. H. He, Q. Han, and R. H. Wu, *Appl. Phys. Lett.* **84**, 5100 (2004).
- ³M. Kondow, K. Uomi, A. Niwa, T. Kitatani, S. Watahiki, and Y. Yazawa, *Jpn. J. Appl. Phys., Part 1* **35**, 1273 (1996).
- ⁴P. Sundgren, J. Berggren, P. Goldman, and M. Hammar, *Appl. Phys. Lett.* **87**, 071104 (2005).
- ⁵M. Amiotti, G. Guizzetti, M. Patrini, L. Francesio, P. Franzosi, G. Mattei, and G. Landgren, *Semicond. Sci. Technol.* **10**, 492 (1995).
- ⁶A. Ulyanekov, U. Klemradt, and U. Pietsch, *Physica B* **248**, 25 (1998).
- ⁷M. Mitsuhashi, M. Ogasawara, and H. Sugiura, *J. Cryst. Growth* **210**, 463 (2000).
- ⁸J. Tersoff, *Phys. Rev. Lett.* **56**, 632 (1986).
- ⁹J. T. Titantah, D. Lamoen, M. Schowalter, and A. Rosenauer, *J. Appl. Phys.* **101**, 123508 (2007).
- ¹⁰J. C. Woicik, J. A. Gupta, S. P. Watkins, and E. D. Crozier, *Appl. Phys. Lett.* **73**, 1269 (1998).
- ¹¹J. C. Woicik, J. G. Pellegrino, B. Steiner, K. E. Miyano, S. G. Bompadre, L. B. Sorensen, T.-L. Lee, and S. Khalid, *Phys. Rev. Lett.* **79**, 5026 (1997).
- ¹²T. L. Lee, M. R. Pillai, J. C. Woicik, G. Labanda, P. F. Lyman, S. A. Barnett, and M. J. Bedzyk, *Phys. Rev. B* **60**, 13612 (1999).
- ¹³J. C. Woicik, *Phys. Rev. B* **57**, 6266 (1998).
- ¹⁴A. Amore Bonapasta and G. Scavia, *Phys. Rev. B* **50**, 2671 (1994).
- ¹⁵J. Massies and N. Grandjean, *Phys. Rev. Lett.* **71**, 1411 (1993).
- ¹⁶O. Lazarenkova, P. von Allmen, S. Lee, F. Oyafuso, and G. Klimeck, *Proceedings of the 12th International Symposium Nanostructures: Physics and Technology*, St. Petersburg, Russia, 2004 (unpublished).
- ¹⁷O. Lazarenkova, P. von Allmen, F. Oyafuso, and S. Lee, *Appl. Phys. Lett.* **85**, 4193 (2004).
- ¹⁸S. Lee, O. L. Lazarenkova, P. von Allmen, F. Oyafuso, and G. Klimeck, *Phys. Rev. B* **70**, 125307 (2004).
- ¹⁹J. Stangl, V. Holy, and G. Bauer, *Rev. Mod. Phys.* **76**, 725 (2004).
- ²⁰D. M. Bruls, J. Vugs, P. Koenraad, H. Saleminck, J. H. Wolter, M. Hopkinson, M. Skolnick, F. Long, and S. P. A. Gill, *Appl. Phys. Lett.* **81**, 1708 (2002).
- ²¹O. Stier, M. Grundmann, and D. Bimberg, *Phys. Rev. B* **59**, 5688 (1999).
- ²²S. Schulz and G. Czycholl, *Phys. Rev. B* **72**, 165317 (2005).
- ²³J. Y. Laval, S. Kret, C. Delamarre, P. Bassoul, T. Benabbas, and Y. Androussi, *Microsc. Microanal.* **8**, 312 (2002).
- ²⁴O. Brandt, K. Ploog, R. Bierwolf, and M. Hohenstein, *Phys. Rev. Lett.* **68**, 1339 (1992).
- ²⁵F. Ishikawa, M. Hóricke, U. Jahn, A. Trampert, and K. H. Ploog, *Appl. Phys. Lett.* **88**, 191115 (2006).
- ²⁶S. H. Wei and A. Zunger, *Phys. Rev. Lett.* **76**, 664 (1996).
- ²⁷F. Boscherini, C. Lamberti, S. Pascarelli, C. Rigo, and S. Mobilio, *Phys. Rev. B* **58**, 10745 (1998).
- ²⁸T. Hammerschmidt, P. Kratzer, and M. Scheffler, *Phys. Rev. B* **77**, 235303 (2008).
- ²⁹J. C. Woicik, J. O. Cross, C. E. Bouldin, B. Ravel, J. G. Pellegrino, B. Steiner, S. G. Bompadre, L. B. Sorensen, K. E. Miyano, and J. P. Kirkland, *Phys. Rev. B* **58**, R4215 (1998).